Annex 5: FUNMIN: final report

The **FUNMIN** project has been subsidized through ACT (EC Project no. 691712), by the Department for Business, Energy & Industrial Strategy (BEIS), together with extra funding from NERC and EPSRC research councils (UK), ADEME (FR), and MINECO-AEI (ES).

1. Identification of the project and report

Project title	**FUN**damental Studies of **MIN**eral Carbonation with Application to CO_2 Sequestration (**FUNMIN**)
Project ID	299668
Coordinators	Dr Devis Di Tommaso & Dr Greg Chass
Project website	http://research.sbcs.qmul.ac.uk/d.ditommaso/funmin/
Reporting period	October 2019 – March 2023

Participants

Organization	**Main contacts + E-mail**	**Role in the project**
Queen Mary University of London (QMUL)	Dr Devis Di Tommaso d.ditommaso@qmul.ac.uk Dr Greg Chass g.chass@qmul.ac.uk	Coordinators
Cambridge Carbon Capture (CCC)	Mr Michael Evans michael.evans@cacaca.co.uk	Industrial partner
University of Granada (UGR)	Prof. Encarnación Ruiz Agudo encaruiz@go.ugr.es	Academic partner
University of Oviedo (UO)	Prof. Pedro Domingo Alvarez Lloret pedroalvarez@uniovi.es	Academic partner
Université Grenoble Alpes (UGA)	Dr German Montes-Hernandez german.montes-hernandez@univ-grenoble-alpes.fr	Academic partner
Utrecht University (UU)	Prof. Mariette Wolthers M.Wolthers@uu.nl	Academic partner

2. Executive summary

FUNMIN, a project led by QMUL (UK), aimed to optimize the process of CO_2 mineralization into added-value Mg-carbonates ($MgCO_3$). The project used a synergy between simulation and experiment to resolve the molecular events surrounding $MgCO_3$ formation: Mg^{2+} dehydration, $MgCO_3$ nucleation, and growth. FUNMIN was conducted in collaboration with the industrial partner Cambridge Carbon Capture Ltd, a company developing technologies to mineralize CO_2 gas into value-added Mg-carbonates, and academic partners in Spain, France, and The Netherlands with a record of accomplishment in geochemical modelling (UU, NL), spectroscopy (UGA, FR), imaging (UGR. ES), and structural analysis (UO, ES).

The specific objectives of FUNMIN and related research work packages (WPs) were:

- **Objective 1:** To characterize of the reaction mechanism and kinetics of the rate-determining Mg-dehydration process in a series of solutions, in order to resolve the catalytic role of composition in promoting $Mg^{2+}\cdots H_2O$ dissociation (*WP1: Mg^{2+} dehydration*).
- **Objective 2:** To determine of the nucleation pathway & the role of solution composition on the formation and stability of anhydrous and hydrated $MgCO_3$ pre-nucleation clusters, in order to reveal the variables promoting the selective formation of anhydrous $MgCO_3$ (*WP2: $MgCO_3$ nucleation*).
- **Objective 3:** To identify the molecular processes at solid-liquid interfaces, and the roles of solution composition & surface nano-morphology, in promoting the growth of anhydrous $MgCO_3$ (*WP3: Magnesite growth*).
- **Objective 4:** To identify what catalyses the direct CO_2 conversion to anhydrous $MgCO_3$ at mild conditions and how it occurs, through a fundamental understanding of the mechanisms controlling the thermodynamics and kinetics of Mg-dehydration, $MgCO_3$ nucleation, and Magnesite growth (*WP4: Practical upscaling*).
- **Objective 5:** To manage the day-to-day and strategic activities of the project including communication within the consortium and external collaborations, and to promote the results through publications and presentations (*WP5: Management and dissemination*).

The FUNMIN project has managed to contribute to both the fundamental understanding of the CO_2 mineralization process, the development of computational and technologies to track the CO_2-to-$MgCO_3$ conversion process, and initiated work to use the generated carbonates as value-added construction materials. The **main achievement** of the project are:

- **Achievement 1:** The research team identified the molecular mechanism that leads to the formation of $MgCO_3$ from solution, including the elementary step that controls the rate-determining Mg-dehydration process and the solution conditions that can accelerate this process.
- **Achievement 2:** FUNMIN, in collaboration with CCC, the Rutherford Appleton Laboratory (RAL), and Modern Age Plastics (MAPS), developed CO_2 mineralization reactors to convert CO2 into MgCO3. They used state-of-the-art neutron beams to conduct in-situ analyses of the process in real-time.
- **Achievement 3:** The resulting carbonates were used to make concrete blocks that met or exceeded international standards (ISO-1920-4). This “green” alternative could potentially replace cement powder and sequestering CO_2 in the process.

3. Role and contributions of each project partners

Table 3.1: Role of each project partner in the FUNMIN project.

Partner	Role and contributions in each WP
QMUL	The QMUL team (Devis Di Tommaso, Greg Chass, Dimitrios Toroz, Fu Song) used atomistic simulation techniques and spectroscopic measurements to reveal the elementary processes that control Mg-dehydration, MgCO3 nucleation, and growth. They also developed CO2 mineralization reactors with CCC, RAL, and MAPS, and managed the project.
	WP1 QMUL developed and conduct atomistic simulations of aqueous electrolyte solutions to characterize the reaction pathways for the Mg-dehydration process, the kinetics of $Mg\cdots H_2O$ dissociation in a series of solutions, and the low-frequency (0–1200 cm^{-1}) dynamical response of water molecules in the Mg^{2+} hydration shell. These simulations were complemented by THz measurements of ultrafast ((sub)pico seconds) dynamics of H_2O around Mg^{2+} ions as a function of solution composition.
	WP2 Using atomistic simulations, the QMUL team revealed the reaction pathways for the $MgCO_3$ clusters formation in solution using at methods. Computational tools to predict the structure & thermodynamic stability $MgCO_3$ nuclei as a function of size, hydration, solution composition was also developed. Neutron Compton Scattering and *in-situ* WANS/SANS experiments were also conducted to track particle formation during $MgCO_3$ nucleation from solution were conducted at the Rutherford Appleton Lab (UK).
	WP3 QMUL performed molecular dynamics (MD) simulations of structurally heterogeneous magnesite surfaces in the presence and absence of catalytic ions were also conducted. QENS experiments were used to track damping of H_2O dynamics (translation, rotation) at magnesite surfaces in contact with electrolyte solutions. Controlling hydration of magnesite to generate other phases with applied uses.
	WP4 QMUL designed and built CO_2 mineralization reactors to convert CO_2 into $MgCO_3$. They collaborated with RAL and CC to develop in-situ analytical instruments to track the CO_2 mineralization in real-time using state-of-the-art neutron beams. The resulting carbonates were used to make concrete blocks and mechanical testing were conducted to verify their performance compared to (ISO-1920-4).
	WP5 QMUL was primarily responsible for managing the project and coordinate the dissemination of the results.
CCC	The team of CCC (Michael Evans, Robert Copcutt, Antony Cox), a leading developer of commercial mineral carbonation technology, worked closely with QMUL to modify their experimental set-up to observe the reaction of CO_2 with solid Mg sources and the formation of carbonates
	WP4 The CCC have co-designed a high-precision flow cell for the neutron scattering observation of CO_2 mineralization. This instrument now provides a real-time, in-situ "window at RAL where users could examine CO_2 mineralization reactions under realistic operating conditions.

UGR	The UGR team (Encarnacion Ruiz-Agudo and Francesco Santoro) contributed to the FUNMIN project by using their expertise in the following areas: The structure of mineral surfaces; Fluid-mineral interactions; The influence of organic and inorganic additives on the growth of crystals in multicomponent aqueous solution.	
UGR	WP2	UGR conducted titration experiments coupled with *in situ* DLS to measure the time evolution of free [Mg^{2+}] in a carbonate solution, in the absence and presence of different amounts of additives, to analyse particle size of $MgCO_3$ clusters formed in solution. Morphological analysis of prenucleation $MgCO_3$ clusters using high-resolution TEM.
UO	The UO team (Pedro Alvarez-Lloret) contributed to the FUNMIN project by using their expertise in the characterization of the chemical composition and crystalline properties of mineral replacement reactions at low temperature. They used X-ray diffraction techniques to study the chemical and structural mechanisms that control the growth and transformation of mineral phases.	
	WP3	UO conducted solid-state X-ray diffraction and pair distribution function analysis to characterise the hydrated, amorphous, and crystalline phases of Mg-carbonates to identify the nucleation and growth pathway of $MgCO_3$.
UGA	The UGA team, led by German Montes-Hernandez, has made available to the FUNMIN consortium their time-resolved Raman spectrometer (785 nm) at UGA. The spectrometer was designed and developed by the team to follow mineral precipitation reactions in-situ.	
	WP2	Solution speciation and chemical characterization of hydrated and anhydrous nucleating particles were conducted using the time-resolved in-situ Raman spectroscopy set-up developed at UGA under changing solution conditions.
UU	THE UU team (Mariette Wolthers) has contributed through her experience in molecular dynamics (MD) on mineral-water interfaces and MD output post-processing for the development of macroscopic geochemical models.	
	WP3	Development of macroscopic analytical geochemical models for magnesite specific surface complexation modelling to predict surface reactivity.

4. Description of activities and final results

The **timeline** of the FUNMIN project and associated work packages are described in **Table 4.1**. A description of the main activities and results is then reported for each WP of the project.

Table 4.1: Work package list.

WP	WP title	Lead	Participants	Start	End
WP1	Mg^{2+} dehydration	QMUL	QMUL, UGA	1	28
WP2	$MgCO_3$ nucleation	QMUL	UGR, UGA	10	28
WP3	$MgCO_3$ growth	QMUL	UO, UGR, UU	21	30
WP4	Practical upscaling	QMUL	QMUL, CCC, RAL	9	36

WP1: Mg-dehydration.

Summary: We have developed and applied a wide range of atomistic simulation methods, including quantum chemistry (QC), molecular dynamics (MD), and free energy (FE) methods, to investigate the reaction mechanism and kinetics of the rate-determining Mg-dehydration process in a series of solutions. These simulations revealed, for the first time, the catalytic role of composition in promoting Mg···H_2O dissociation. The simulations were complemented by low-frequency THz and neutron scattering experiments.

Deliverables: **D1.1** Computational models and tools to describe ion-water Mg^{2+} interaction. **D1.2** Water exchange reaction pathways around Mg^{2+}. **D1.3** Report on water exchange around Mg^{2+} as a function of solution composition. **D1.4** Report on the low-frequency H_2O dynamics around Mg^{2+}.

Deviations from work plan: n/a

D1.1 Computational models and tools to describe ion-water Mg^{2+} interaction. The accuracy of the potential model employed in classical MD is critical for meaningful simulations of Mg^{2+} solutions and $MgCO_3$-solution interfaces. Energetic, structural, time-dependent, and kinetic properties have been computed using more than ten interatomic potentials of Mg^{2+} ions in aqueous solutions (2019). Representative results obtained from these simulations and comparison with QC and available experimental data are reported in **Fig. 4.1**. The Lennard-Jones parameters in the general AMBER forcefield has been chosen for subsequent modelling simulations because it provides the best compromise between accuracy and availability for a wide range of organic and inorganic ions. We also developed an atomistic simulation scheme for the determination of the hydration number parameter (*h*) of aqueous electrolyte solutions based on the calculation of the water dipole reorientation dynamics (2020) (**Fig. 4.2**). The application of this protocol gives h values of $MgCl_2$ solutions in excellent agreement with experimental hydration numbers

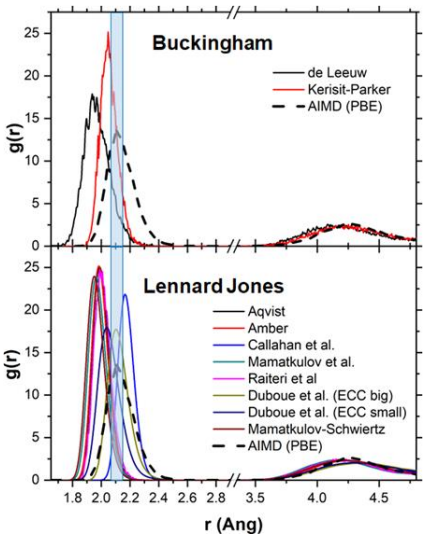

Figure 4.1. Mg–H_2O radial distribution [g(r)] grouped by ion model. Blue vertical line at 2.09 ± 0.04 Å is the experimental position of the 1st shell.

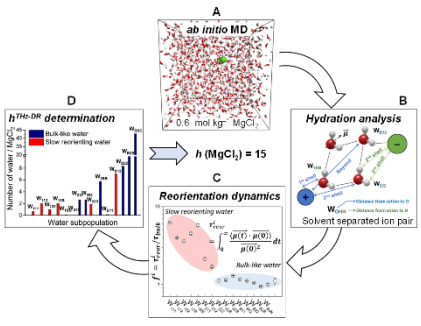

Figure 4.2. Water reorientation dynamics from ab initio MD trajectories and determination of hydration numbers of aqueous electrolytes.

obtained using GHz-to-THz dielectric relaxation spectroscopy (2020). The value of *h* represents the number of water molecules participating in the solvation of the ions and influenced by the presence of the ions and give a measure of the strength of interaction of an ion with the surrounding water molecules. The Mg ion has a significantly higher hydration number than the Ca ion (2022), explaining why Mg-dehydration is rate-determining in the $MgCO_3$ nucleation.

D1.2 Water exchange reaction pathways around Mg^{2+}. In **Fig. 4B**, the free energy profiles of hydrated Mg^{2+} as a function of the ion–water coordination number are compared to that of Ca^{2+}. For Ca^{2+}, the seven-coordinate $Ca(H_2O)_7^{2+}$ is the most likely hydration state, contrasting with the 6-coordinate preference of Mg^{2+}; six- and eight-coordinate states are also accessible for Ca^{2+} at room temperature (**Fig. 4.1**, in blue). Ca^{2+} incorporation in Ca-carbonates may occur through dissociative (7→6) or associative (7→8) pathways. The hydrated Mg^{2+} has a very stable minimum for six-fold coordination with water, $Mg(H_2O)_6^{2+}$, whilst the five-coordinated intermediate, $Mg(H_2O)_5^{2+}$, is inaccessible at 300 K (due to a high activation barrier between six- and five-coordinated states) (2020). H_2O exchange is drastically retarded in the first hydration shell of Mg^{2+}, hence why precipitate rates of $MgCO_3$ are six orders of magnitude slower than $CaCO_3$ at 300 K.

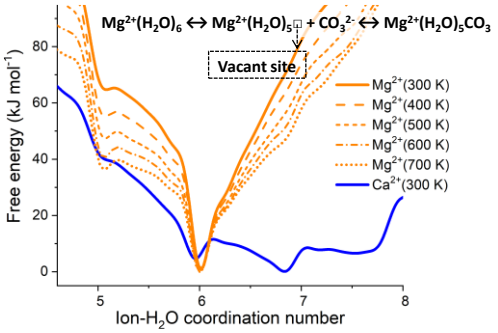

Figure 4.3. Free energy profiles of hydrated Ca^{2+} and Mg^{2+} as a function of the ion-water coordination number.

D1.3 Water-exchange rates around Mg^{2+} as a function of solution composition. We have developed a computational procedure to characterise the effect of solution additive anions on the mechanism of Mg^{2+}–H_2O dissociation (2021). Anions such as bisulfide, carboxylate and fluoride ions can stabilise undercoordinated Mg^{2+} hydration configurations, even when they are in the second hydration shell of Mg^{2+} (**Fig. 4.4A)** QC wavefunction analyses revealed the changes in bonding responsible for the equilibration of five and six hydrated states, with insight into the mechanisms by which these can inter-change and open-up coordination sites on the central Mg^{2+} ion (**Fig. 4.4B**). The characterisation of the rate determining Mg^{2+} dehydration process in a series of solutions, as covered in our work, contributes to resolving the catalytic role of solution composition in promoting Mg^{2+} dehydration, and subsequent $MgCO_3$ formation in natural and industrial environments. The results of this work were featured on the cover of the journal CrystEngComm and were selected for its hot-article collection.

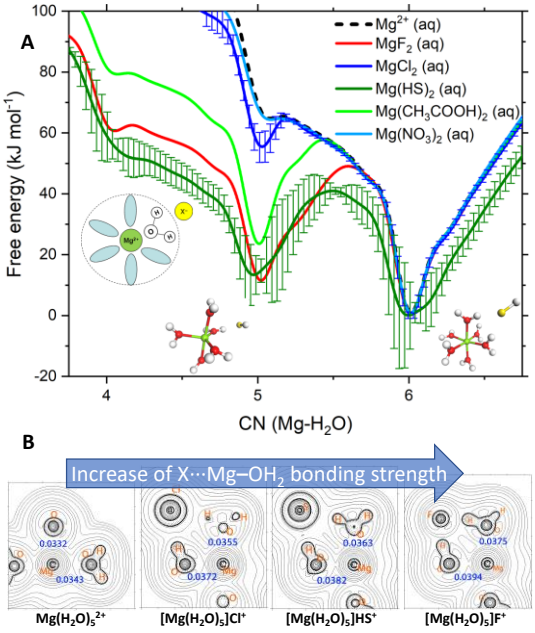

Figure 4.4. (A) Free energy as a function of the Mg^{2+}-H_2O coordination number, CN(Mg-H_2O), for hydrated Mg^{2+} (single Mg^{2+}, no counterions) and solvated Mg^{2+} with a counterion in the second hydration shell. The structures are the five- and six-coordinated states in $Mg(HS)_2$(aq). **(B)** 2-D Laplacians of electronic density ($\nabla^2\rho$) in the plane of the Mg, O, H and X atoms in $Mg(H_2O)_5^{2+}$ and $[Mg(H_2O)_5]\cdot X^+$ (X = F^-, Cl^-, HS^-).

D1.4 Characterization of low-frequency H_2O dynamics around Mg^{2+}. Neutron scattering measurements (@RAL) and THz spectroscopy (@NPL) revealed the effect of ions on water dynamics. **Figs. 4(a-c)** shows quasi elastic neutron scattering (QENS) at the ISIS neutron facility at RAL (UK). **Fig. 4(a)** show the spectra of $MgCl_2$ (aq) and $Mg(CH_3COOH)_2$ (aq) at different concentrations. The immobile hydrogen index in **(c)** is related to the Mg wt.% and increases with higher Mg concentration. **Fig. 4(d)** reports THz Absorbance Coefficient among $MgCl_2$ and MgSO4 solutions characterize low-frequency H_2O dynamics around Mg^{2+}. The focus has been on generating time-dependent profiles over minutes and hours of the reaction products emerging from bulk reactors, and thus directly related to the

industrial processes. The averaged changes over these timescales provide a window on the phase changes ongoing over the course of these processes, as well as a glimpse into their evolving mechanical properties.

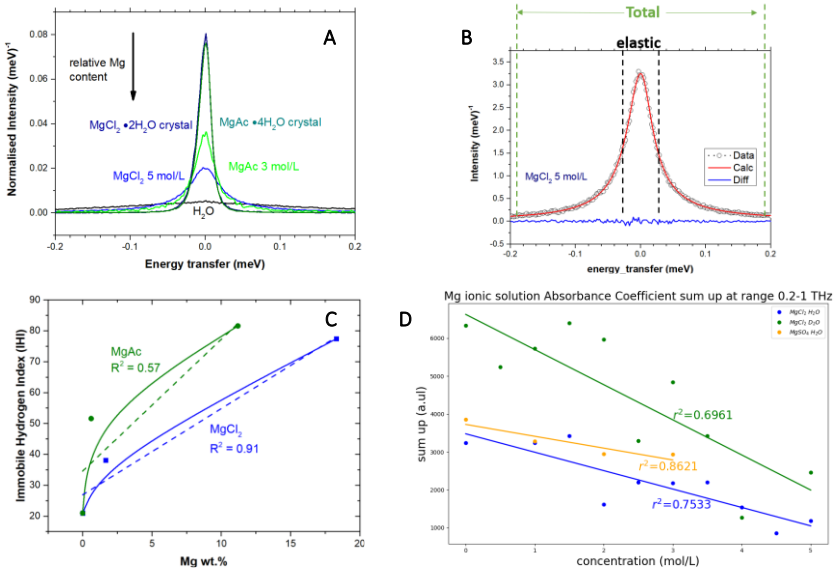

Figure 4.4. (a-c) QENS at the ISIS neutron facility at RAL (UK). **(a)** show the spectra of $MgCl_2$ (aq) and $Mg(CH_3COOH)_2$ (aq) at different concentrations. The immobile hydrogen index in **(c)** is related to the Mg wt.% and increases with higher Mg concentration. **(d)** THz Absorbance Coefficient among $MgCl_2$ and MgSO4 solutions characterize low-frequency H_2O dynamics around Mg^{2+}.

WP2: $MgCO_3$ nucleation.

Summary: We have developed a computational database based on well-defined molecular-level criteria to determine which solution additives promote the nucleation of $MgCO_3$. Time-resolved Raman experiments have confirmed that the presence of ions containing carboxylic groups, such as acetate, in solution promotes the formation of magnesite at relatively low temperatures. We have also determined the nucleation pathway leading to the formation of $MgCO_3$: prenucleation clusters form within a few microseconds, which is the first evidence of the existence of prenucleation clusters of $MgCO_3$ in solution. These clusters then form amorphous hydrated nanoparticles, which then assemble to crystallize into needlelike, micrometer-sized crystals of nesquehonite.

Deliverables: **D2.1** Computational database of solution additives promoting Mg^{2+} dehydration and $MgCO_3$ nucleation. **D2.2** Simulation of $MgCO_3$ aggregation as a function of solution composition. **D2.3** Characterization of phase changes during aqueous $MgCO_3$ formation. **D2.4** Particle size and chemical characterization of $MgCO_3$ pre-nucleation clusters (PNCs) with solution composition. **D2.5** Tracking of solution crystallisation using neutron scattering.

Deviations from work plan: n/a

D2.1 Computational database of solution additives promoting Mg^{2+} dehydration and $MgCO_3$ nucleation. Extensive atomistic simulations of the rate determining $Mg^{2+}\cdots H_2O$ dissociation were conducted to characterize the ability of thirty additives to promote Mg^{2+} dehydration based on well-defined molecular level criteria (**Fig. 4.4**): (i) Form solvent shared ion pairs or contact ion pairs with Mg^{2+} that are less stable than $Mg^{2+}\cdots CO_3^{2-}$; (ii) Stabilize undercoordinated hydrated Mg^{2+} states with a vacant coordination site to which CO_3^{2-} can bind initiating $MgCO_3$ nucleation or Mg^{2+} incorporation into the crystal lattice; (iii) Weaken the "hydration cage" formed by the water molecules in the first shell of Mg^{2+}. Through a fundamental understanding of the role of solution composition to the Mg^{2+} dehydration mechanism, our computational database (2022) may help identifying the solution composition conditions catalyzing the low-temperature CO_2 conversion into $MgCO_3$.

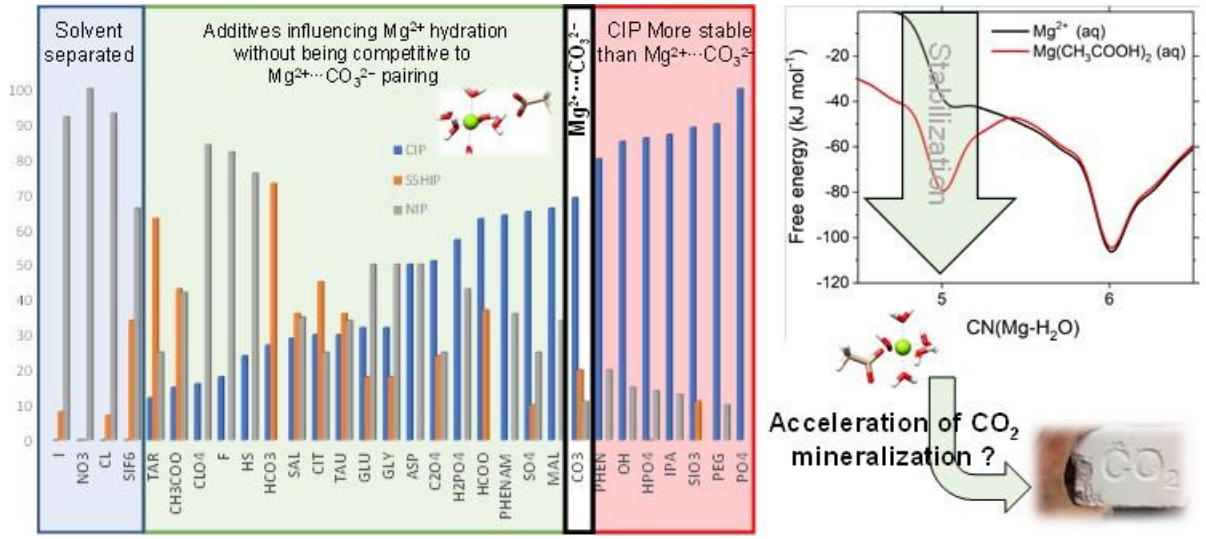

Figure 4.4. We investigated the influence of solution additive anions on the early stages of MgCO3 nucleation. We computed the Mg^{2+} and anions pairing to reveal the propensity to inhibit or promote $Mg^{2+}\cdots CO_3^{2-}$ formation. We determined the stabilization of undercoordinated hydrated Mg^{2+} states to which CO_3^{2-} can bind. We simulated the aggregation of $MgCO_3$ clusters in the presence of additives.

D2.2 Simulation of $MgCO_3$ aggregation as a function of solution composition. Atomistic models and computational procedures based on classical MD were developed to simulate aqueous electrolyte solutions containing Mg^{2+} and CO_3^{2-} ions in the *absence* and *presence* of non-crystalline anions (CH_3COO^-, SO_4^{2-}, Cl^-, $C_2O_4^{2-}$) and cations (Na^+, Li^+). We simulated the process of $MgCO_3$ aggregation from solution; formation of prenucleation clusters can be observed within the timeframe of few µs, which is the first evidence of the existence of prenucleation clusters (PNC) of $MgCO_3$ in solution The effect of solution additives has also been considered (**Fig. 4.5**). There is a significant effect of solution additives on the hydration level of the $MgCO_3$ cluster (water molecules directly coordinated to Mg^{2+}) (2022). Dehydration occurs according to the following order: $CO_3^{2-} > CH_3COO^- > Cl^-$. This agrees with *in-situ* Raman measurements (**D2.3**), showing that the presence of acetate promotes the generation of anhydrous $MgCO_3$.

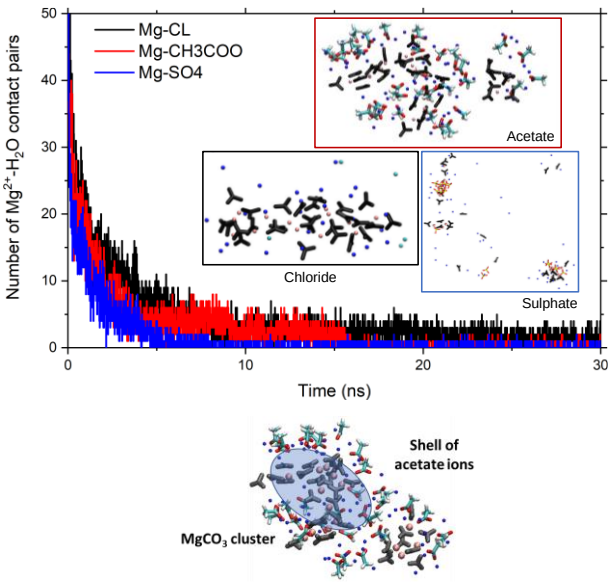

Figure 4.5. Progressive contact pairs of Mg^{2+} with O atoms of H_2O. Snapshots of $MgCO_3$ clusters forming in the presence of acetate, chloride, and sulfate ions

D2.3 Report on phase changes during aqueous $MgCO_3$ formation. Time-resolved Raman experiments were conducted to characterise the phase change during the formation of Mg-carbonates (**Fig. 4.6**). Based on the results of the computational database of solution additives promoting Mg^{2+} dehydration, the measurements were conducted under different solution conditions (CH_3COO^-, SO_4^{2-}, NO_3^-). The presence of acetate ions in solution promotes magnesite ($MgCO_3$) formation, which occurred at T = 90°C, considerably lower than the temperatures necessary to observe $MgCO_3$ crystallization in "pure" water conditions (mixing of $MgCl_2$ and $NaCO_3$) or reported in the literature (120 < T < 185 °C, P > 100 atm, Chem. Eng. Sci., 2008, 63, 1012). We explain this accelerating effect in terms of the ability of CH_3COO^- ions to stabilize undercoordinated Mg^{2+} hydration configurations, opening coordination sites on the central Mg^{2+} ion and promoting the formation of Mg-carbonates (2021). QC analyses also shows changes in bonding responsible for the equilibration of five and six hydrated states, with insight into the mechanisms by which these can inter-change and open-up coordination sites on the central Mg^{2+} ion (2021).

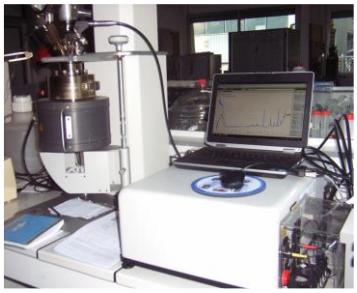

Experimental setup for time-resolved Raman spectroscopy at UGA to monitor nucleation and growth

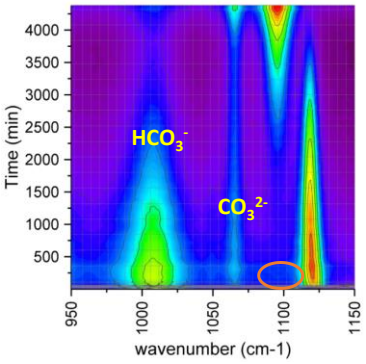

$Mg(CH_3COOH)_2$ @ 90 C

$MgCl_2.7H_2O$ (aq) + $NaCO_3$ (aq) → $MgCO_3 \cdot 3H_2O$ (s) T = 90 °C (stable hydrated phase)

$Mg(CH_3COO)_2$ (aq) + $NaCO_3$ (aq) →

$MgCO_3 \cdot 3H_2O$ (s) → $Mg_5(CO_3)_4(OH)_2 \cdot 4H_2O$ (s) → $MgCO_3$ (s), T = 90 °C (fast)

Figure 4.6. Summary of time-resolved Raman measurements at Grenoble of phase changes during the aqueous $MgCO_3$ formation from mixing $Mg(CH_3COOH)_2$ (aq) + Na_2CO_3 (aq) at 90 °C. The presence of acetate ions facilitates the formation of the anhydrous $MgCO_3$.

D2.4 Particle size and chemical characterization of $MgCO_3$ PNCs with solution composition. Morphology, structure and vibrational spectra of magnesium carbonate hydrates synthesized by slow titration of $MgCl_2$ into a K_2CO_3 solution was studied by FESEM, TEM, FT-IR, XRD and TGA. Precipitation experiments were performed using a Titrino 905 (Metrohm) in a jacketed vessel at controlled temperature (25ºC±0.2ºC) and under continuous stirring. A 100 mM $MgCl_2$ solution was continuously added to a 50 mM K_2CO_3 at a rate of 0.2mL min^{-1}. $MgCl_2$ and K_2CO_3 solutions were prepared from 0.1 M stock solutions made from solids from Sigma Aldrich ($MgCl_2 \cdot 6H_2O$, min. 99.995% and K_2CO_3, min. 99%) and doubly deionized water (Milli-Q, resistivity <18.2 MΩ cm). During the titration experiments, the pH was measured using a glass electrode from Methrom. Transmittance was monitored with Optrode sensor for titration using wavelength of 520 nm (Metrohm) in order to detect the onset of crystallization. After the experimental runs, the solids were filtered through cellulose nitrate membrane filters (Millipore, pore size = 0.2 µm) and quickly immersed in liquid nitrogen for subsequent vacuum drying at -50ºC using Telstar LyoQuest. This was done (1) once the transmittance was stabilized after the initial drop showing the onset of crystallization -initial precipitates- and (2) 24 h after the onset of crystallization -final precipitates-. Solids were then investigated by attenuated total reflectance-Fourier transform infrared spectroscopy frequency range 400-4000 cm^{-1}; 2 cm^{-1} spectral resolution) equipped with an attenuated total reflectance (ATR-FTIR; Jasco Model 6200). Additionally, a fraction of the solids was deposited on zero-background Si sample holders and analyzed by X-ray diffraction using a PANanalytical X'Pert ProX-ray diffractometer equipped with Cu Kα radiation (λ=1.5405 Å) at 2θ range between 3 and 70°and at a scanning rate of 0.017°2θs^{-1}. Furthermore, the solids were subjected to simultaneous TG and DSC analysis on a Mettler-Toledo. About 10–20 mg of the sample was deposited on Al crucibles and analyzed under flowing N_2 (100 mL/min) at 20 °C /min heating rate, from 25ºC to 950 °C. The particles were carbon coated prior to analysis by field emission scanning electron microscopy (FESEM, Zeiss SUPRA40VP) equipped with energy dispersive X-ray analysis (EDX), and transmission electron microscopy (TEM) using a FEI Titan, operated at 300 kV. Prior to TEM observations, freeze-dried solids were re-suspended in ethanol and deposited on carbon film coated copper grids. TEM observations were performed using a 30 µm objective aperture, which is a compromise between amplitude and phase contrast images. Selected area electron diffraction (SAED) images were collected using a 10 µm objective aperture. Such aperture allows collection of diffraction data from a circular area of 0.5 µm diameter. **Fig. 4.7A** provides a set of typical FESEM images corresponding to the precipitates sampled at different reaction times. As it can be observed, the initial precipitates consist of aggregates of spherical nanoparticles of

50-100 nm in size (**Fig. 4.7A** - first panel). In some areas, these nanoparticles seem to align and coalesce to form 100-nm thick fibers (**Fig. 4.7A** - second panel). Such fibers seem to be the precursor of the needle-like crystals of micrometer size found in the precipitates obtained upon long contact time with the precipitating solution (**Fig. 4.7A** - third panel 1c). This needle-like morphology is commonly reported for nesquehonite ($MgCO_3 \cdot 3H_2O$). However, a detailed observation of these needlelike particles as shown in the high magnification (**Fig. 4.7A** – fourth panel) show that the smooth surfaces seen at lower magnification are composed of spherical nanoparticles with a diameter below 100 nm. TEM observations and associated SAED patterns confirm that the nanoparticles in the initial precipitates are of amorphous character (**Fig. 4.7B**). *X-Ray diffraction (XRD).* Characteristic XRD patterns of initial (red plot) and final (blue plot) precipitates can be seen in **Fig. 4.7C**. The absence of peaks in this pattern confirms the amorphous character of the initial precipitates, as already detected by TEM analysis. Only a very broad band, centered around 30 º2θ, is observed. Contrarily, the diffractogram corresponding to the final precipitates show intense and narrow peaks all consistent with the reported pattern of nesquehonite ($MgCO_3 \cdot 3H_2O$), in agreement with the observed morphology described above. Based on the results of this inverstigation, it can be concluded that (i) the first phase formed in the system appears as amorphous nanoparticles with a general formula of $MgCO_3 \cdot 1.37\ H_2O$; (ii) these nanoparticles are prone to assemble and crystallize into needlelike, micrometer-sized crystals, and (iii) although IR vibrational spectra and XRD pattern of the final needlelike crystals indicate that the phase formed is nesquehonite, a significant proportion of amorphous material initially coexist with the crystalline phase, as suggested by the average formula of $MgCO_3 \cdot 1.74\ H_2O$ determined by TGA for the needlelike precipitates.

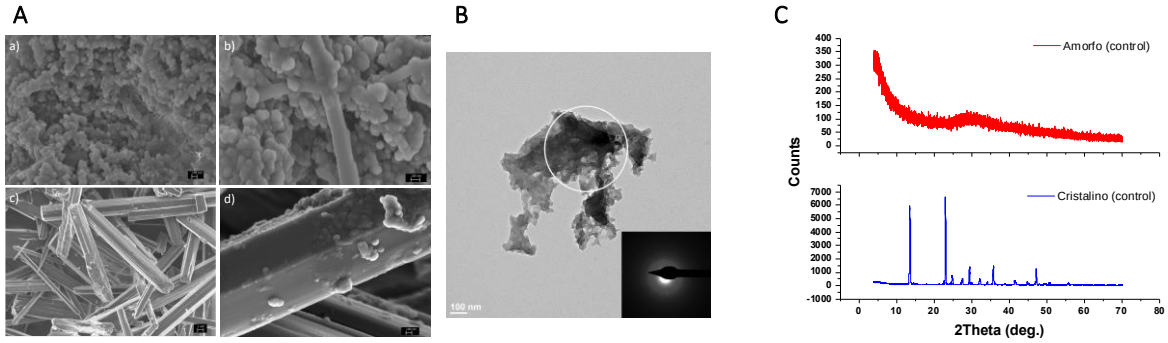

Figure 4.7. (A) TEM images and **(B)** electron diffraction pattern of amorphous MgCO3 formed in nucleation experiments. **(C)** XRD patterns of solids collected at the end of the MgCO3 nucleation compared with the crystalline phase.

D2.4 Tracking of solution crystallisation using neutron scattering. We conducted the 1st ever Neutron Compton scattering measurements of any crystallization, completed 01-06 March 2020 at the RAL-ISIS facility (UK). These measurements have been instrumental in helping advance the accurate tracking of solution crystallization; early stages of Mg-dehydration and nucleation. Measurements were conducted using the VESUVIO (Compton scattering) experimental setup at RAL on the following systems solution and solid phase systems: $Mg(CH_3COO)_2$, $Mg(OH)_2$ and $MgCO_3 \cdot 3H_2O$ **Fig. 4.8a** reports the raw spectra generated during the allocated time. Currently, we have also developed tools to deconvolute the spectra and quantify experimentally, for the first time, the role of solution composition on "weakening" the local Mg-water interaction. The industrial partner, CCC, visited RAL (**Fig. 4.8b**) to attend the experiments and initiate the discussion for the design of a flow-cell for neutron scattering with the QMUL team and RAL teams (**D4.4** in WP4).

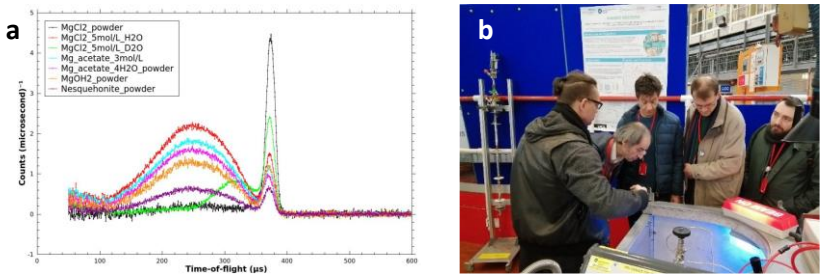

Figure 4.8. (a) Compton scattering spectra in time of flight from VESUVIO. **(b)** Tuesday 3rd March 2020: visit of the Cambridge Carbon Capture at RAL-ISIS laboratories during the Compton scattering experiments.

WP3: $MgCO_3$ growth.
Summary: We used heterogeneous atomistic models of $MgCO_3$–water interfaces and molecular dynamics simulations to simulate the elementary processes controlling the early stages of $MgCO_3$ growth. Our simulations revealed that the solution composition and surface nanomorphology play a significant role in promoting the growth of $MgCO_3$. These simulations were complemented by synchrotron XRD experiments to characterize the phase composition and crystal structure of the products obtained from the nucleation experiments conducted in WP2.
Deliverables: D3.1 Computational report on magnesite surface reactivity. **D3.2** Solid state characterization of magnesite.
Deviations from proposal/ work plan: n/a

D3.1. Computational report on magnesite surface reactivity. Atomistic models of magnesite interacting with aqueous solutions were built and molecular dynamics simulations were conducted to determine the water exchange around the Mg ions (the rate-determining step of $MgCO_3$ growth) (**Fig. 4.10**). The simulations revealed that the surface site type (face, edge, corner, etc.) and composition have a significant impact on the kinetics of this process. The structural data (Mg-water distances, hydrogen bonds) obtained from the simulations will be used to develop a site-specific surface complexation model that can be used to describe the chemical structure and charging behavior of distinct surface sites, and to predict the concentration of growth sites needed for ion-by-ion growth.

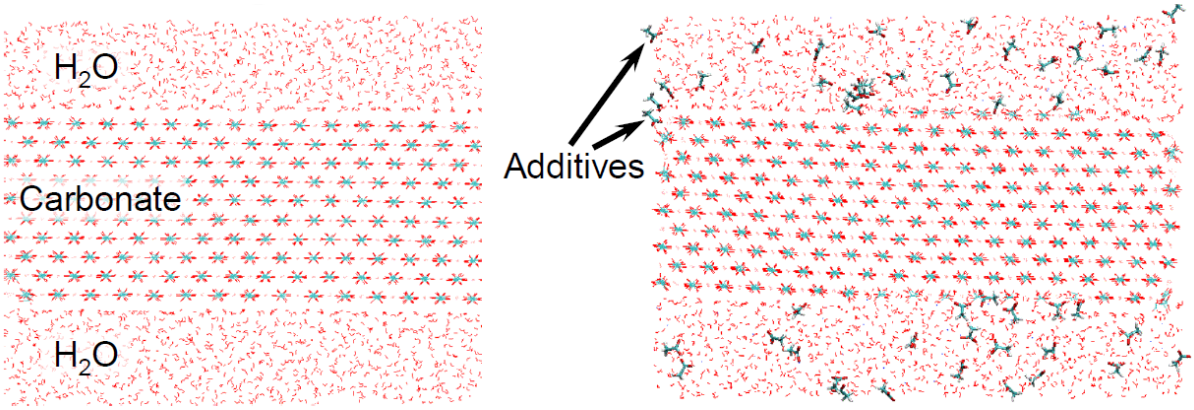

Figure 4.10. Simulations of the $MgCO_3$ growth on the (101-4) cleavage plane –a particular orientation of the surface of the mineral – in the absence (**left**) and presence (**right**) of additives (acetate). Simulations also including such features as terraces, steps and other sites were considered.

D3.2. Solid state characterization of metal-doped magnesite. The synchrotron XRD experiments were measured at the high-resolution Materials Science and Powder Diffraction (MSPD) beamline at ALBA (Barcelona, Spain). The diffraction patterns were acquired using a MYTHEN position-sensitive detector. The wavelength λ = 0.952729Å, was selected with a double-crystal Si (111) monochromator. The powder material was filled in Ø = 0.7 mm borosilicate capillaries (Hilgenberg GmbH, Germany) and an empty capillary was measured for background corrections. The capillaries were rotated during data collection to improve diffracting particle statistics. The data acquisition time was ~ 30 min per pattern over the angular range 1–35° (2θ). A LaB_6 standard material (NIST SRM 660b) was measured under the same conditions to obtain the instrumental resolution. The K-factor (instrument intensity constant) was applied to determine amorphous contribution on the SXRD pattern (O'Connor, 1988). The crystallographic parameters and amorphous/crystalline phase fraction (percentages) were obtained by the Rietveld method using the HighScore Plus 4.1 software package. The phase composition and crystal structure of the precipitates were measured by high-resolution SXRD. **Fig. 4.11** displays the profile fit calculated from the SXRD patterns of the different crystalline and amorphous (associated with the presence of a background) phases of the analyzed samples. The percentage of each crystalline/amorphous phase as well as structural information, including crystalline parameters for the cell parameters obtained by the Rietveld fitting, are summarized in

Table 1. The results indicate a high amorphous magnesium carbonate content (around 90%) and the simultaneous precipitation of magnesium carbonate hydrated (i.e., nesquehonite: 8.4%; hydromagnesite: 0.8%) and anhydrous (magnesite: 0.2%) crystalline phases. Cell parameters according to space group indicate structural variations of the identified crystalline phases. The variation in the content of water molecules and hydroxyl ions was accompanied by a structural alteration of the hydrated magnesium carbonate phases. These crystalline parameters reported in Table 2 were compared with the values obtained for nesquehonite (a = 7.72100(12) Å, b = 5.37518(7) Å, c = 12.1430(3) Å, β = 90.165(4)°) and hydromagnesite (a = 10.12175(5) Å, b = 8.9536(3) Å, c = 8.3886(2) Å, β = 114.372(4)°). These results agree with FESEM, TEM, FTIR and TGA observations (**D2.3**). The spherical nanoparticle aggregates observed in the initial precipitates correspond with the major presence of AMC (amorphous phase), also corroborated with TEM observations. The presence of other crystalline phases is also observed in these precipitates, predominantly nesquehonite and in a smaller proportion another hydrated (hydromagnesite) and anhydrous (magnesite) phases of magnesium carbonate. The ATR-FTIR results also demonstrate the formation of these hydrated and anhydrous phases of magnesium carbonate. The variation in the hydration formula of these phases, observed with TG analyses, may be due to the coexistence of these hydrated magnesium carbonate phases as well as possible intermediate stable phases during the thermal analytical process. In conclusion, the structural formula of nesquehonite were identified as $MgCO_3 \cdot 3H_2O$, according to the IMA. On the other hand, nesquehonite, acts as a precursor to hydromagnesite, which is the most common hydrated magnesium carbonate at atmospheric CO_2 pressure within the temperature range typical of most surface environments (Hopkinson et al., *Geochim. Cosmochim. Acta*, 2012, 76, 1–13.). This mineral transformation is achieved through one or more stages of dissolution-precipitation steps, involving a variety of phases metastable intermediates such as the dypingite-type phase, $Mg_5(CO_3)_4(OH)_2 \cdot xH_2O$ (x = 5, 6, 8, 11).

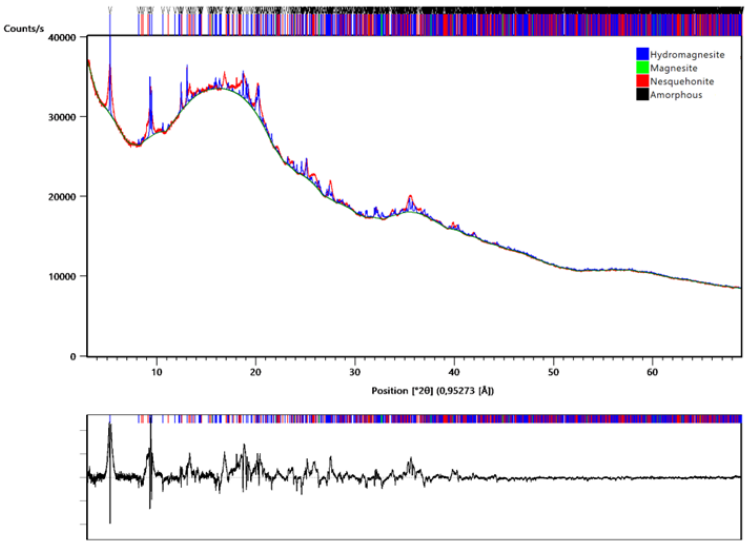

Figure 4.11. Rietveld refinement on synchrotron radiation diffraction (SRD) patterns.

Figure 4.11. Rietveld refinement details adjustment.

Rietveld parameters	*Values calculated* (%)
R expected	0.71862
R profile	1.49402
Weighted R	2.36298
D-statics	0.05259
Weighted D	0.06099
Goodness of fit	2.28823

WP4: Practical upscaling.

Summary: We designed and built two generations of reactors to test and optimize CO_2 mineralization under industrial conditions. We collaborated with the CCC and RAL to generate schematics from which a prototype was constructed for a carbonation rig that performs in-situ neutron measurements of $MgCO_3$ formation from solution. We used the generated Mg-carbonates from the CO_2 mineralization process to make concrete blocks and conducted compressive strength measurements to verify they meet the international standards (ISO-1920-4).

Deliverables: D4.1 First generation bulk CO_2 mineralization reactor: design and fabrication. **D4.2** Second generation reactor: 10+kg / hour bulk mineralisation. **D4.3** Flow-cell for neutron scattering measurements of CO_2 mineralization: engineering schematics, construction, and testing. **D4.4** In situ tracking of CO_2 mineralization: neutron spectra. **D4.5** Carbonated cements: generation and performance testing.

D4.1 First generation bulk CO_2 mineralization reactor: design and fabrication. We designed and built-up generation reactors to test and optimize CO_2 mineralization under industrial conditions. The 1st generation (**Fig. 4.11**) was a 10L simplistic cylindrical design with a central helical spiral (to provide mineralization surfaces) and an impeller through the center to action-controlled mixing. Successful in the production of ~1-2 kg of output carbonates/hour, the reactor had issues of inhomogeneity throughout the reactor.

Fig. 4.11. 1st generation CO_2 mineralisation

D4.2 Second generation reactor: 10+kg/hour bulk mineralisation. The limitations of the 1st generation reactor were remedied in the 2nd generation (**Fig. 4.12**) where a bottom 3-way valve (to pump or output to filtration) allowed for pumping the reaction mixture and homogenizing the reaction. An overall hexagonal reactor shape and central helical structure was improved with sharper angles and closely spaced "blades". Evidence of success is the accelerated agglomeration and growth of the output carbonates in stalactite-type structures (**Fig. 4.12**). This reactor scaled up the CO_2-to-$MgCO_3$ conversion to ~10-20kg. This reactor was developed together with Modern Age Plastics (MAPS, Canada). Major improvements arose from the pumping, homogenizing reactants, as well as optimization of central helical blade geometries. These resulted in improved aggregation and growth of carbonate outputs not on top of the helical blades, but also hanging from and growing downwards, in 'stalactite-like' structures.

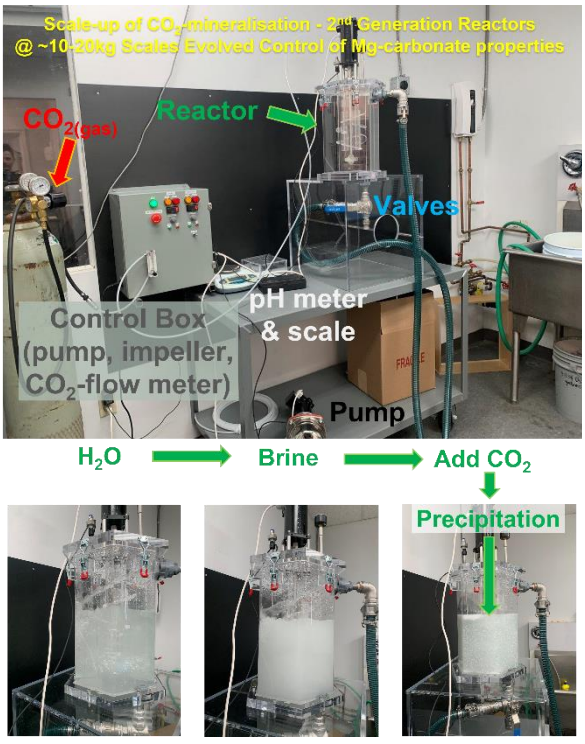

Fig. 4.12. 2nd generation CO_2 mineralization reactor.

D4.3 Flow-cell for neutron scattering measurements of CO_2 mineralization: engineering schematics, construction, and testing. The industrial partner CCC developed a carbonation rig to observe the reaction of CO_2 with various solids, such as $Mg(OH)_2$, and the formation of Mg-carbonates in an aqueous slurry (**Fig. 4.13(a)**). However, such a simple experimental set-up has a serious of limitations: it only allows ex-situ analysis of the generated $MgCO_3$ samples. Together with CCC, the QMUL team set the ambitious task of designing and constructing a prototype rig (**Fig. 4.13(b)**). to enable

batched or continuous sampling of the slurry in a high precision flow cell for performing spectroscopic *in situ* characterization of real-time CO_2 mineralization from aqueous environments at the ISIS neutron center, RAL facility (**Fig. 4.13(c)**). The QMUL team has secured additional funding from the "Impact Acceleration Account" (£25,000) to develop the proposed CO_2 mineralization rig. In the period Oct 2020 – June 2021, the QMUL, CCC, and RAL teams have worked on the initial conceptual design of the flow cell: 1) Research interface designs and space envelopes of the various test cells at RAL; 2) Background experiment to determine the most appropriate design philosophy and gas/liquid contactor concept; 3) Develop design concept for review by the QMUL team. Weekly engineering and design meetings between QMUL, CCC and RAL led to the production of detailed engineering schematics to realise our concept for an *in-situ* CO_2-mineralisation rig consisting of a pressure resistant and radiation safe rig including a reaction chamber, sample flow-cell, waste-dump and requisite pumps & shielding to be utilised on the Vesuvio (NCS) and IRIS (QENS) neutron beamlines. In May 2021, after 9 months of work the prototype was tested in the RAL-UK facilities (**Fig. 4.14(e)**). The details of the development of the flow-cell for neutron scattering measurements published (2022).

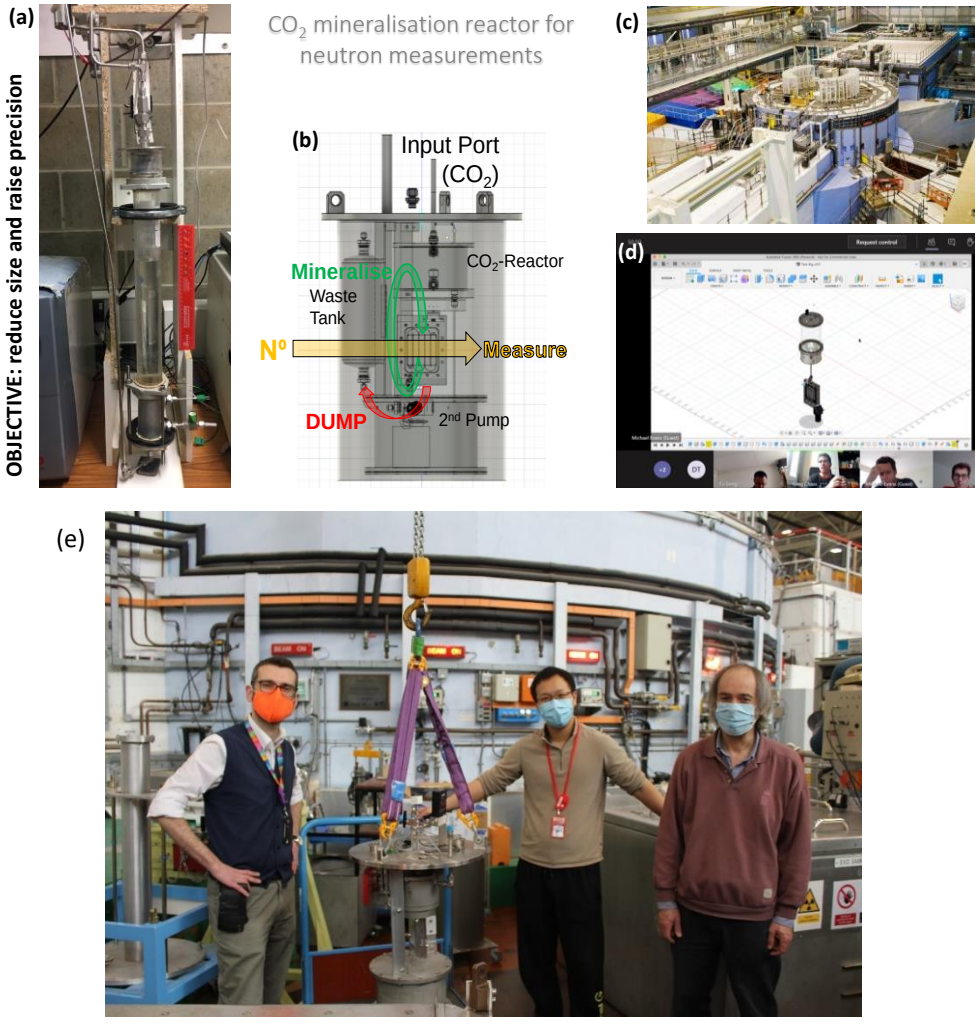

Fig. 4.13. (a) Original prototype industrial reactor to track the permanent sequestering of $CO_{2(g)}$ by $Mg(OH)_2$; **(b)** Proposed initial design of high-precision flow cell for real time, in situ neutron scattering observation of CO_2 mineralization at the **(c)** UK's neutron and muon facility of the Rutherford Appleton Laboratory. **(d)** 3D model and Engineering Design Specification of the flow cell discussed during the August 2020 FUNMIN meeting. **(e)** Dr Giovanni Romanelli (RAL), Dr Fu Song (QMUL), and Dr Robert Copcutt (Cambridge Carbon Capture) with the rig next to the Vesuvio instrument (RAL, UK).

D1.4 In-situ tracking of CO_2 mineralization in real-time. We employed the flow cell developed in **D1.3** to conduct in-situ scattering of Mg-containing aqueous slurries reacting and sequestering CO_2(g) (**Fig. 3**). This relevant reactor has allowed us to track the course of reaction over min and hrs of the transformations of aqueous slurry and gaseous-CO_2 to Mg-carbonates. The slurries were filled into the

reaction chamber after which pre-determined masses/volumes of CO_2(g) were introduced via a helical nebulization valve. Preliminary empty-instrument and empty-cell measurements provided calibration baselines of the background, whilst sample-transmission runs identified optimal scattering settings - between data-collection efficacy and multiple-scatter. On-the-fly analyses tracked the changes to the sample as well as identified any potential problems arising, including valve or pipe blockages, pump-inefficiencies, or failure. Once changes to relevant variable became negligible, the reactions were deemed concluded and the measurements stopped. Once determined as safe to remove from the beamline, the mineralization rig was placed into lead-housing until no longer 'radioactively hot' enough to be inspected, opened, re-inspected, and subsequently cleaned. Three time-dependent variables were tracked to gauge rection progression: CO_2-usage, neutron transmission (tracks density change), neutron scattering (tracks bonding changes thus mineralization). Preliminary results indicate non-monatomic progression of the reaction, with some oscillations in the Compton profiles of both H- and Mg-atoms. This identifies key times in the industrial transformations where the process may be most readily improved and optimized.

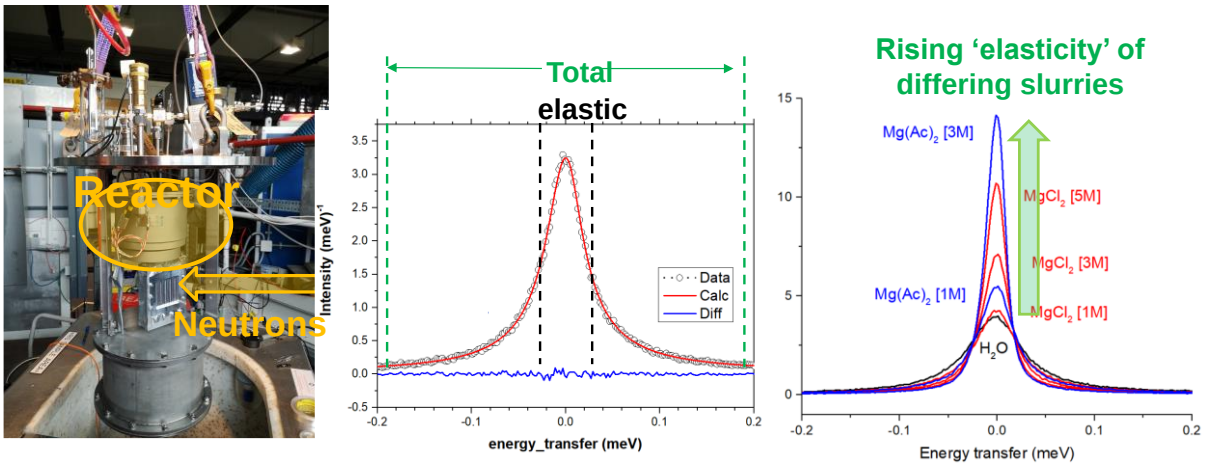

Fig. 4.14. (Left) Flow cell to conduct in-situ scattering of Mg-containing aqueous slurries reacting and sequestering CO2(g) at RAL (UK). **(Centre)** Quasi-elastic scattering provides real-time tracking of viscosity ongoing. **(Right)** Differing 'elasticity' values for the sample are related to differing bulk viscosity and aggregation present and evolving.

D4.5 Carbonated cements: generation and performance testing. The Mg-carbonates outputs from the bulk reactor (**D4.1** and **D4.2**) carbonates were used in making concrete blocks satisfying and surpassing international standards (ISO-1920-4, Fig. **4.15**), relevantly and profitably replacing cement powder whilst sequestering CO_2. Tests were conducted at CONSELAB (Rome, IT) to provide the necessary measure of concrete performance as well as routes to optimization. The goal was to produce carbonated concrete that is superior in performance to other concrete products on the market, such as bricks or pavers (between 32.5 and 42.5 MPa, depending on application). This deliverable represents a proof of process and concept for 'novel concrete mix'.

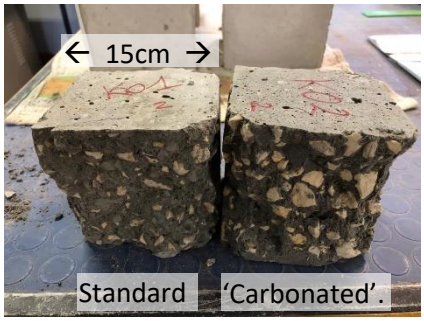

Fig. 4.15. Compressive strength tests on **OUR concretes** (2022-Oct samples, CONSELAB) with the $MgCO_3$ generated using 1st generation CO_2 mineralization reactor. *Left*, standard concrete block. *Right,* Mg-carbonate filled block with ~2% Mg-carbonate (thus 0.8g CO_2).

Financial summary table

The table below gives an account of the budgets spent by the partners per work package.

Partner	WP1	WP2	WP3	WP4	WP5	Total	Actual % of total grant
QMUL	116,223	142,638	126,789	116,223	26,414	528,288	100%
UGR		54,631	40,973	13,658	6,829	116,090	100%
Oviedo			98,817	9,882	4,941	113,640	100%
UGA	30,476	38,095		7,619	3,810	80,000	100%
TOTAL	146,699	235,364	266,579	147,382	41,994	838,018	100%

5. Project impact

Table 5.1: Impact of the key results achieved by the FUNMIN project.

Type of impact	Key result	Implication	Status
Contribution to the facilitation of the emergence of CCUS	The presence of anions, such as fluoride and carboxylate, can stabilize undercoordinated hydration configurations of Mg ions, which can lower the barrier to dehydration and subsequent incorporation into the lattice of Mg-carbonates. This can promote the formation of low-temperature $MgCO_3$.	Our discovery of Mg-dehydration processes in natural systems has implications for geochemistry and CO_2 mineralization technologies. Slow $MgCO_3$ precipitation from solution is a challenge, but our findings could lead to new strategies for accelerating precipitation and sequestering CO_2.	Results published in *CrystEngComm* (2021), *Cryst. Growth Des.* (2022) and presented in several conference and invited seminars.
Contribution to the facilitation of the emergence of CCUS	Nucleation pathways & the role of solution composition on the selective nucleation of anhydrous and hydrated forms of $MgCO_3$ identified.	The first-principles simulations and advanced experimental techniques of the mechanisms controlling $MgCO_3$ nucleation aqueous solution has led to the identification of factors that can catalyse magnesite formation under mild conditions *mild*, *non-hazardous*, and *non-toxic* conditions: T = 90 in the presence of acetate ions under *mild*, *non-hazardous*, and *non-toxic* conditions.	Joint publication between QMUL, UGR, UO and UGA in preparation. Preliminary results presented in several conference and invited seminars.

Contribution to the facilitation of the emergence of CCUS	New technology to track CO_2 mineralization developed.	The high-precision flow cell for in-situ, real-time neutron scattering experiments developed during the FUNMIN project could initiate a new line of research into CO_2 mineralization. This research could help to bridge the gap between fundamental science at neutron source centers such as RAL (UK) and the carbonate materials and cement industry.	We have demonstrated the viability of the instrument through several experiments in 2021 and 2022. The manuscript reporting the design of the technology ca be found here and its publication is currently in the second stage of review.
Chances for commercializing the technology further		Concrete blocks made from carbonates meet or exceed international standards (ISO-1920-4, Fig.3). This could potentially replace cement powder while also sequestering CO2. Tests on carbonated concrete blocks conducted at CONSELAB have shown comparable or superior mechanical performance to other concrete products on the market, such as bricks or pavers (between 32.5 and 42.5 MPa, depending on application).	A follow-up grant proposal for the commercialization of an integrated process to mineralize low-value brines into high-value carbonates for the cement industry has passed the outline stage and is currently under review.

6. Implementation

Relevance of the FUNMIN to the ACT objective of accelerating & maturing CCS technology.

Annual CO_2 capture is approximately 40 million tonnes per year (Mt/yr) and is growing exponentially. In the UK alone, it is expected to reach 130 Mt by 2050. (Greenhouse gas removal, The Royal Society, 2018). With concerns about CO_2 loss through seepage and its subsequent environmental effects, CO_2 storage and utilization, especially, is becoming increasingly important. CO2 mineralization into $MgCO_3$ could offer a highly profitable and fully scalable approach for CO2 storage and utilization, with the following advantages:

- High density CO_2 storage: 1.6 tonnes CO2/m3 for MgCO3, twice as large as supercritical CO_2.
- Huge capacity of feedstock minerals/waste options worldwide containing Mg ions.
- Wide application in the cement industry, where carbonate-based construction materials are estimated to reach annual revenues of $1 trillion by 2030 (MI CCUS Workshop, 2017).

The main barriers to the commercial deployment of CO_2 mineralization are high energy intensity, low reaction conversion, and slow reaction rates. Despite being an exothermic process (energy-releasing) and thus thermodynamically favourable, the CO_2-to-$MgCO_3$ mineral carbonation process is kinetically slow. According to the **Utilization Panel Report: CO_2 Conversion to Solid Carbonates** (Mission Innovation CCUS Workshop, 2017), the performance of CO_2 mineralization technologies is hindered by the current lack of fundamental molecular scale understanding of the processes controlling mineral carbonation. The FUNMIN project has addressed this challenge by: Identifying the elementary step that controls the rate-determining Mg-dehydration process (**D1.2** and **D1.3**); Determining the mechanism of formation of $MgCO_3$ from solution (**D2.2**, **D2.4**, and **D3.2**); Determining the solution conditions that can accelerate CO2-to-MgCO3 conversion (D2.1 and D2.3).

FUNMIN also addressed the priority thematic area **Carbonation of Industrial Wastes with CO_2** in the **Research and Innovation (R&I) Activity 7: CCU Action**, to deliver **Target 8** ("*new technologies for the production of fuels, value added chemicals and/or other products from captured CO_2*"**)** of the SET-Plan TWG9 CCS and CCU Implementation Plan (2017). Carbonation processes can be applied to a range of Mg-rich industrial mineral wastes and by-products (e.g., brines) as well as Mg-silicate deposits, but to bridge the gap between lab-scale pilots and pre-commercial pilots R&I Activity 7 highlights the need to develop "*more efficient CO_2 valorisation process technologies*". The design of the flow cell for neutron scattering measurements of CO_2 mineralization (**D4.3** and **D4.4**) represents a unique tool for tracking CO_2 conversion to carbonates in real time and obtaining experimentally atomic-level resolution of the elementary processes controlling this event under industrially relevant conditions.. Moreover, our preliminary results from mechanical testing of carbonated cements (**D4.5**) show that the Mg-carbonates outputs from the bulk reactor (**D4.1** and **D4.2**) have the potential to be used profitably to replace cement powder while sequestering CO_2.

Engagement with other partners. The collaborative work conducted by FUNMIN has expanded beyond the original academic partners to include other industries and research institutes throughout the project.

- **Rutherford National Laboratory** (UK)**.** We worked very closely with the engineering team at RAL headed by Dr Stewart Parker, one of the UK leading specialists in neutron science. This collaboration led to the design and build the flow cell for neutron scattering measurements.
- **National Physics Laboratory** (UK). We worked with Dr Mira Naftaly, Senior Researcher at NPL, to expand our experimental characterization to include to THz observation of the ultrafast dynamics of H_2O around ions.
- **Seoul National University** (SK). We have collaborated with the group of Prof Gun-Sik Park, member of the EAB, to develop a combined methodology based on *ab initio* MD and GHz-to-THz dielectric relaxation spectroscopy to determine the hydration number of aqueous electrolyte

solutions, a parameter that specifies the number of water molecules in an electrolyte solution participating in the solvation of the ions and influenced by the presence of the ions (*Phys. Chem. Chem. Phys.*, 2020, 22, 16301; *ChemPhysChem* 2020, 21, 2334– 2346).

- **Canadian universities and industry.** We have created new links with the highly ranked universities **McMaster** and **University British Columbia**, and with the company **Modern Age Plastics** to design the 2nd generation bulk CO_2 mineralization reactors (**D4.2**). These were made of polymethyl pentene due to its chemical inertness, thermal/pressure stability and transparence allowing visual observation of the industrial transformations.
- **Conselab** (IT): Specialists in concrete testing and optimization, construction, and materials procurement consulting. They provided us with their facilities to test the mechanical properties of our carbonated concrete.
- **HeidelbergCement.** After the second virtual workshop organised by Accelerating CCS Technologies, Andrew Burns, Head of Decarbonization and Process Innovation at HeidelbergCement, approached us to discuss the design of our CO_2 mineralization reactor. They have expressed strong interest in a possible collaboration but need to see more data before committing.

7. Collaboration and coordination within the Consortium

Coordination and collaboration. FUNMIN was gathered around a core team at QMUL with the support of world-class expertise from different European laboratories: UGR, UO, UGA and NN. The QMUL coordinators liaised between the partners and the ACT, monitored the various obligations of the network, which includes preparation of the reports that need to be submitted to the ACT and the UK funding body (BEIS), monitored the financial health of the network, organized scientific meetings within and outside the consortium. QMUL has an experienced EU unit, which supported the coordinators in the financial and administrative aspects of FUNMIN. This set-up resulted to be very efficient in conducting the planned research and has minimized the divergence of the scientific and financial aspects of the project caused by the Covid-19 pandemic. We maintained a close collaboration between the members of the consortium members through *regular* meetings, which have been held monthly. The purpose of such meetings was to monitor the research progress, ensure its viability in the light of developments in the fields, and decide upon any necessary changes to the project plans. The industrial partner CCC has been involved in *all* aspects of the project, particularly in WP4; their technical team has significantly contributed to redesigning their carbonation rig into a prototype for high precision and real-time neutron measurements of CO_2 mineralization. An external advisory board consisting high profile academics (Prof Christine Putnis, Prof Denis Gebauer, Prof Gun-Sik Park) and industrialists (Dr Christopher Godwin, Unilever) is also monitoring the progress of the consortium from an external perspective.

8. Dissemination activities

Table 8.1: List of publications and dissemination activities. Type of publication: SPa = Peer reviewed Paper, PPa = Popular science presentation, Pat= Patent application, Po = Poster, OPa = Oral presentation and paper, PoPa = Poster and Paper, O = Oral Presentation, Web = Webinar, WS = WorkShop, V = Video, A = Abstract, B = Blog, I = Interview, PR = Press Release, Oth = Other, please specify.

Type of publication	Authors	Title	Reference	Date/year	Project partners involved	Others involved
SPa	G. Montes-Hernandez, F. Renard	Nucleation of Brushite and Hydroxyapatite from Amorphous Calcium Phosphate Phases Revealed by Dynamic In Situ Raman Spectroscopy	J. Phys. Chem. C, 124, 28, 15302	06/2020	Grenoble	University of Oslo
SPa	X. Wang, D. Toroz, S. Kim, S. Clegg, G. Park, D. Di Tommaso	Density functional theory based molecular dynamics study of solution composition effects on the solvation shell of metal ions	Phys. Chem. Chem. Phys., 2020, **22**, 16301-16313	07/2020	QMUL	Seoul National Univ., East Anglia Univ.
SPa	L. Monasterio-Guillota, P. Alvarez-Lloret, A. Ibañez-Velasco, A. Fernandez-Martinez, E. Ruiz-Agudo, C. Rodriguez-Navarro	CO_2 sequestration and simultaneous zeolite production by carbonation of coal fly ash: Impact on the trapping of toxic elements	Journal of CO_2 Utilization, 2020, **40**, 101263	08/2020	Granada, Oviedo, Grenoble	
SPa	S. Kim, X. Wang, J. Jang, K. Eom, S. L. Clegg, G.-S.	Hydrogen bond structure and	ChemPhysChem, 2020, **21**, 2334	08/2020	QMUL	Seoul National Univ., East

	Park, and D. Di Tommaso	low-frequency dynamics of aqueous electrolyte solutions: hydration numbers from ab initio water dipole reorientation dynamics and dielectric relaxation spectroscopy				Anglia Univ.
SPa	H. C. Cove, D. Toroz, and D. Di Tommaso	The effect of the oxidation state of the metal center in metalloporphyrins on the electrocatalytic CO2-to-CO conversion: A density functional theory study	Molecular Catalysis, 2020, **498**, 111248	10/2020	QMUL	University of Oslo, University of Munster, Curtin University
SPa	MG Guren, CV Putnis, G Montes-Hernandez, HE King, F Renard	Direct imaging of coupled dissolution-precipitation and growth processes on calcite exposed to chromium-rich fluids	Chemical Geology, 2020, **552**, 119770	10/2020	UGA	
SPa	G Montes-Hernandez	Synthesis of magnetite, ceria and magnetite-ceria materials by calcination of nanostructur	Materials Letters, 2020, **276**, 128246	06/2020	UGA	

		ed precursor-minerals				
Web	D. Di Tommaso	FUNdamental Studies of MINeral Carbonation with Application to CO_2 Utilisation	Thomas Young Centre Online Seminar, invited talk	30th April 2020	QMUL	
Web	X. Wang	DFT based molecular dynamics study of aqueous solutions: hydration numbers from ab initio dynamics and THz-DR	CCDC Crystal Conversations, contributed talk	6th August 2020	QMUL	Seoul National Univ.
Web	D. Di Tommaso	Modelling Electrolyte Solutions and Processes of Crystal Growth and Nucleation	SRM Institute of Science and Technology, invited talk	7th July 2020	QMUL	
Web	D. Di Tommaso	FUNdamental Studies of MINeral Carbonation with Application to CO2 Utilisation	Virtual Computational Chemistry Seminar, Cardiff University, invited talk	30th October 2020	QMUL	
Popa	Pedro Alvarez-Lloret, E. Ruiz-Agudo	Crystallographic control characterization during mineral replacement using integrated 2D-X ray diffraction patterns	GE3C 2021	21 Jan 2021	UO, UGR	

SPa	D. Toroz, F. Song, G. Chass, and D. Di Tommaso	New insights into the role of solution additive anions in Mg2+ dehydration: implications for mineral carbonation	Phys. Chem. Chem. Phys., 2020,22, 16301-16313 (Hot Article)	17th March 2021	QMUL	
Spa	M.Yamamoto, K. Takahashi, M. Ohwada, Y. Wu, K. Iwase, Y. Hayasaka, H. Konaka, H. Cove, D. Di Tommaso, K. Kamiya, J. Maruyama, and F. Tani	Iron porphyrin-derived ordered carbonaceous frameworks	Catalysis Today, 2021, **364**, 164-171	15th March 2021	QMUL	Tohoku University
SPa	H. Han, G. Gordeev, D. Toroz, D. Di Tommaso, S. Reich, and B. Flavel	Endohedral Filling Effects in Sorted and Polymer-Wrapped Single-Wall Carbon Nanotubes	*J. Phys. Chem. C* 2021, **125**, 13, 7476–7487	30th March 2021	QMUL	Frei University Berlin, Karlsruhe Institute of Technology
SPa	S. D. Midgley, D. Di Tommaso, D. Fleitmann, R. Grau-Crespo	Sulphur and Molybdenum Incorporation at the Calcite-Water Interface: Insights from Ab Initio Molecular Dynamics	ACS Earth Space Chemistry, 2021, **5**, 2066–2073	7th May 2021	QMUL	University of Reading, University of Basel
Web	D. Di Tommaso	FUNdamental Studies of MINeral Carbonation with Application to CO2 Utilisation	Samarra International Conference for Pure and Applied Sciences, University of Samarra, Samarra, Iraq	23h March 2021	QMUL	

Spa	G. Montes-Hernandez, N. Findling, F. Renard	Direct and Indirect Nucleation of Magnetite Nanoparticles from 2 Solution Revealed by Time-Resolved Raman Spectroscopy	Crystal Growth & Design, 2021, **21**, 3500–3510	29 April 2021	UGR	University of Oslo
Spa	X. Wang, S. L. Clegg, D. Di Tommaso	Bridging atomistic simulations and thermodynamic hydration models of aqueous electrolyte solutions	Journal of Chemical Physics, 2022, **156**, 024502	21 December 2021	QMUL	East Anglia Univ.
Web	D. Di Tommaso	Solution additives promoting the onset of $MgCO_3$	University of Leeds, invited seminar	8 Dec 2021	QMUL	
Oth (preprint)	T. Rao, W. Yuan, N. Jeyachandran, A. G. Nabi, D. Di Tommaso and C. Giordano	Study on the structure vs activity of designed non-precious metal electrocatalysts for CO2 conversion	ChemRxiv, 2021, DOI: 10.33774/chemrxiv-2021-5prsn	17 August 2021	QMUL	
Spa	M. Yamamoto, Z. Qi, S. Goto, Y. Gu, T. Toriyama, T. Yamamoto, H. Nishihara, A. Aziz, R. Crespo-Otero, D. Di Tommaso, M. Tamura, K. Tomishige, T. Kyotani, and K. Yamazaki	Porous nanographene formation on γ-alumina nanoparticles via transition-metal-free methane activation	Chem. Sci., 2022,13, 3140-3146	22 Feb 2022	QMUL	Tohoku Univ., Kyushu University

Oth (preprint)	A. Ghulam Nabi, A. ur Rehman, A. Hussain and D. Di Tommaso	Ab initio random structure searching and catalytic properties of copper-based nanocluster with Earth-abundant metals for the electrocatalytic CO2-to-CO conversion	Materials Letters, 2023, **341**, 134167	21 March 2022	QMUL	Pakistan Institute of Engineering and Applied Sciences ,
Spa	D. Toroz, F. Song, A. Uddin, G. Chass, and D. Di Tommaso	Solution additives promoting the onset of MgCO3 nucleation	Cryst. Growth Des., 2022, **22**, 3080–3089	5 April 2022	QMUL	Tohoku Univ., RIKEN Center for Advanced Photonics
Web	D. Di Tommaso	Solution additives promoting Mg^{2+} dehydration and $MgCO_3$ nucleation: Implications for CO_2 mineralization	University of Leeds, invited seminar	12 May 2022	QMUL	
SPa	F. V. Song, B. Yang, D. Di Tommaso, R. S. Donnan, G. A. Chass, R. Y. Yada, D. H. Farrar, and K. V. Tian	Resolving nanoscopic structuring and interfacial THz dynamics in setting cements	Mater. Adv., 2022,3, 4982-4990	16 May 2022	QMUL	Univ. of Chester, Univ. of British Columbia, McMaster Univ., Sapienza University of Rome
SPa	A. G. Nabi, A. ur Rehman, A. Hussain, D. Di Tommaso	Ab initio random structure searching and catalytic	Molecular Catalysis, 2022, **527**, 112406.	30 May 2022	QMUL	Pakistan Institute of Engineering and

		properties of copper-based nanocluster with Earth-abundant metals for the electrocatalytic CO2-to-CO conversion				Applied Sciences
Oth (preprint)	A. Muthuperiyanayagam, G. N. Azeem, A. ur Rehman, D. Di Tommaso	Adsorption, activation, and conversion of carbon dioxide on small copper-tin nanoclusters	ChemRxiv, DOI: 10.26434/chemrxiv-2022-2j73m	1 July 2022	QMUL	Pakistan Institute of Engineering and Applied Sciences
OPa	D. Di Tommaso	Revealing the elementary processes revealing the conversion of small and abundant molecules to added-value chemicals and materials	UK Catalysis Hub Summer Conference 2022	20 & 21 June 2022	QMUL	
OPa	D. Di Tommaso	Solution additives promoting the onset of MgCO3 nucleation and growth.	BACG Annual Conference 2022	28 June 2022	QMUL	
Web	D. Di Tommaso	Revealing the elementary processes controlling the conversion	Huazhong University of Science and Technology, invited seminar	1 July 2022	QMUL	

		of small molecules to added-value materials				
OPa	D. Di Tommaso	Revealing the elementary processes controlling the conversion of CO2 to added-value chemicals & materials	Chemical Process & Energy Resources Institute, Thessaloniki	18 July 2022	QMUL	
SPa	E. Ruiz-Agudo, C. Ruiz-Agudo, C. Lázaro-Calisalvo, P. Álvarez-Lloret, and C. Rodríguez-Navarro	Nanoscale observations of periclase (MgO) hydration	EGU General Assembly 2022, Vienna, Austria, EGU22-12060, https://doi.org/10.5194/egusphere-egu22-12060, 2022.	23-27 May 2022	UGR, UO	University of Konstanz
SPa	E. Ruiz-Agudo, C. Ruiz Agudo, P. Alvarez-Lloret, S. Bonilla-Correa, C. Rodríguez-Navarro	An experimental study of periclase (MgO) hydration	Goldschmidt 2022	16 July 2 2022	UGR, UO	University of Konstanz
SPa	Q. Zhao, M. Yamamoto, K. Yamazakic, Hirotomo Nishihara, R. Crespo-Otero, D. Di Tommaso	The carbon chain growth during the onset of CVD graphene formation on γ-Al_2O_3 is promoted by unsaturated CH_2 ends	Phys. Chem. Chem. Phys., 2022, **24**, 23357-23366	9 Sept 2022	QMUL	Tohoku University , RIKEN Center for Advanced Photonics
SPa	F. V Song, B. Yang, D. Di Tommaso, R.S Donnan, G.A Chass, R. Y Yada, D. H Farrar, K.V. Tia	Resolving nanoscopic structuring and interfacial THz dynamics in setting cements	Mater. Adv., 2022, **3**, 4982-4990	13 May 2022	QMUL	Univ.of Chester, Univ. of British Columbia, McMaster , Sapienza Univ.

Oth (preprint)	A. G. Nabi, A. ur Rehman, A. Hussain, G. Chass, D. Di Tommaso	Optimal Icosahedral Copper-based Bimetallic Clusters for the Selective Electrocatalytic CO2 Conversion to One Carbon Products	Nanomaterials 2023, **13**, 87	17 Nov 2022	QMUL	Pakistan Institute of Engineering and Applied Sciences
Oth (preprint)	A. Mortazavi, F. V. Song, M. Dudman, M. Evans, R. Copcutt, G. Romanelli, F. Demmel, D. H. Farrar, S. F. Parker, K. V. Tian, D. Di Tommaso, and G. A. Chass ChemRxiv, 2022, DOI: 10.26434/chemrxiv-2022-hfxtx	CO2-mineralization and carbonation reactor rig: design and validation for in situ neutron scattering experiments - engineering and lessons learned	doi: 10.26434/chemrxiv-2022-hfxtx	29 Nov 2022	QMUL	Rutherford Appleton Laboratory, Cambridge Carbon Capture, Rutherford Appleton Laboratory, Sapienza University of Rome, The University of British Columbia, University of Rome Tor Vergata
SPa	G. N. Azeem, Aman-ur-Rehman, A. Hussain, G. A. Chass, and D. Di Tommaso	Optimal icosahedral copper-based bimetallic clusters for the selective electrocatalytic CO_2 conversion to one carbon products	Nanomaterials, 2023, **13**, 87.	24 Dec 2022	QMUL	University of Gujrat, Pakistan Institute of Engineering & Applied Sciences

SPa	Q. Guo, Q. Zhao, R. Crespo-Otero, D. Di Tommaso, J. Tang, S. Dimitrov, M. Titirici, X. Li, and A. Jorge Sobrido	Single-Atom Iridium on Hematite Photoanodes for Solar Water Splitting: Catalyst or Spectator?	J. Am. Chem. Soc. 2023, **145**, 3, 1686–1695	11 Jan 2023	QMUL	Imperial College London, University College London, Northwestern Polytechnical University
SPa	M. Qiao, M. Wang, X. Meng, H. Zhu, Y. Zhang, Z. Ji, Y. Zhao, J. Liu, S. Wang, X. Guo, J. Wang, J. Bi, P. Zhang, D. Di Tommaso, F. Li, and J. Yuan	Fine analysis of the component effect on the microstructure of LiCl solution	J. Mol. Liq., 2023, **373**, 121238	9 Jan 2023	QMUL	Hebei University of Technology
SPa	M. S. Salha, R. Y. Yada, D. H. Farrar, G. A. Chass, K. V. Tian, E. Bodo	Aluminium catalysed oligomerisation in cement-forming silicate systems	Phys. Chem. Chem. Phys., 2023, **25**, 455-461	8 Dec 2022	QMUL	Sapienza University of Rome, The University of British Columbia, McMaster University
SPa	H Adenusi, GA Chass, S Passerini, KV Tian, G Chen	Lithium Batteries and the Solid Electrolyte Interphase (SEI)—Progress and Outlook	Adv. Energy Mater.2023, **13**, 2203307	18 Jan 2023	QMUL	Helmholtz Institute Ulm, Sapienza University of Rome, The University of British Columbia, McMaster University, Hong Kong Quantum AI Lab
OPa	G. A. Chass, K. V. Tian, D. Di Tommaso	CO2-Mineralisation to Added	Indo-UK Symposium for Enabling Chemical	19 Jan, 2023	QMUL	Sapienza University of Rome, The

		Value Products: Raising Process Efficacy From Nanoscopic Through Industrial Scales	Technologies for Sustainability			University of British Columbia, McMaster University
SPa	Q. Guo, Q. Zhao, R. Crespo-Otero, D. Di Tommaso, J. Tang, S. Dimitrov, M. Titirici, X. Li, and A. Jorge Sobrido	Single atom iridium on hematite photoanodes for solar water splitting: catalyst or spectator?	J. Am. Chem. Soc. 2023, **145**, 1686–1695	11 Jan, 2023	QMUL	Imperial College London, UCL, Northwestern Polytechnical University
SPa	W. Yuan, N. Jeyachandran, T. Rao, A. G. Nabi, M. Bisetto, D. Di Tommaso, T. Montini, and C. Giordano	Study on the structure vs activity of designed non-precious metal electrocatalysts for CO2 conversion	Materials Letters, 2023, **341**, 134167	4 March 2023	QMUL	University of Trieste
SPa	A. Muthuperiyanayagam, G. N. Azeem, A. ur Rehman, and D. Di Tommaso	Adsorption, activation, and conversion of carbon dioxide on small copper–tin nanoclusters	Phys. Chem. Chem. Phys., 2023, **25**, 13429-13441	19 Apr 2023	QMUL	Pakistan Institute of Engineering & Applied Sciences, University of Gujrat
SPa	Marcos, C., Lahchich, A., Álvarez-Lloret	Hydrothermally treated vermiculites: Ability to support products for CO2 adsorption and geological implications	Applied Clay Science, 2023, **232**, 106791	15 December 2022	UO, UGR	

SPa	Marin-Troya P, Espinosa C, Monasterio-Guillot L, Alvarez-Lloret P.	Carbonate Minerals' Precipitation in the Presence of Background Electrolytes: Sr, Cs, and Li with Different Transporting Anions	Crystals. 2023, **13**, 796	10 May 2023	UO, UGR, UGA	

[a] Roundtable discussion focusing on opportunities and challenges for Carbon Capture and Use (CCU) commercialisation in the Canadian and British markets organised by the Innovation, Science and Economic Development Canada (ISED) and The UK Government's Department for Business, Energy and Industrial Strategy (BEIS).